

## Spirocyclic Peptidomimetics Featuring 2,3-Methanoamino Acids

Dongyeol Lim and Kevin Burgess\*

Contribution from the Department of Chemistry, Texas A &amp; M University, College Station, Texas 77843-3255

Received May 19, 1997<sup>⊗</sup>

**Abstract:** The spirocyclic peptidomimetics cyclo-[(2*S*,3*S*)-cyclo-R]GD[(2*S*,3*S*)-cyclo-R]GD (**3**) and cyclo-[(2*R*,3*S*)-cyclo-R]GD[(2*R*,3*S*)-cyclo-R]GD (**4**), containing 2,3-methanoarginine (cyclo-Arg') residues, were prepared. Conformations of these molecules were studied via a combination of CD and 1D and 2D NMR, and these data were interfaced with extensive molecular simulations. Conformational biases for molecules **3** and **4** were thereby deduced and were compared with conclusions previously obtained (Burgess, K.; Lim, D.; Mousa, S. A. *J. Med. Chem.* **1996**, *39*, 4520) for cyclo-[RGDRGD] (**2**). Molecule **3** has a relatively clear conformational bias toward a structure with a type II  $\beta$ -turn between the Gly CO and Gly NH atoms, but **4** is more flexible, existing in conformers wherein the Asp and Arg side chains tend to be on opposite faces of the backbone cyclic structure. These conclusions were used to interpret the relative affinities of **2–4** with respect to the vitronectin receptor.

Cyclic peptides are often prepared as a prelude to development of pharmaceuticals from linear peptide lead compounds. Joining peptide *N*- and *C*-termini significantly restricts their conformational freedom, often in ways that enforce or preclude bioactive conformations.<sup>1–5</sup> Either of these results, positive or negative, can be informative. It is not easy, however, to confidently predict the conformational effects of such restrictions in advance, and the cyclization event does little to constrain side-chain conformations. New approaches to this old problem, therefore, are desirable.

Our studies of 2,3-methanoamino acids<sup>6,7</sup> led us to speculate about the effects that these would have on cyclic peptidic systems.<sup>8</sup> In small linear peptides, cyclopropyl amino acids restrict the conformations of otherwise flexible systems,<sup>9–14</sup> so in cyclic compounds it seemed logical that they would affect backbone and side-chain conformations simultaneously. We therefore decided to investigate spirocyclic peptides formed from 2,3-methanoamino acids.

Almost any model peptidic system could be used to explore spirocyclic systems containing 2,3-methanoamino acids, but peptides in the RGD series were a logical choice because we had already prepared two stereoisomers of 2,3-methanoarginine.<sup>15</sup> Moreover, there is abundant data on cyclic peptides

containing the RGD sequence<sup>16–28</sup> as a result of the pivotal role of this fibrinogen motif in cell surface interactions.<sup>29</sup> Our preliminary work in this area featured preparation, conformational studies in solution, and biological data for the linear hexapeptide RGDRGD (**1**) and the cyclic hexapeptide cyclo-[RGDRGD] (**2**).<sup>30</sup> Compound **2** was found to adopt a type I  $\beta$ -turn conformation with a relatively short distance between the Asp and Arg side chains. It selectively bound the  $\alpha V\beta 3$  vitronectin receptor in preference to the IIb/ $\beta 3$ -fibrinogen receptor, and this bioactivity may be associated with relatively close Asp/Arg side-chain proximities. Moreover, these observations concerning the conformation and receptor binding proper-

(16) Samanen, J.; Ali, F.; Romoff, T.; Calvo, R.; Sorenson, E.; Vasko, J.; Storer, B.; Berry, D.; Bennett, D.; Strohsacker, M.; Powers, D.; Stadel, J.; Nichols, A. *J. Med. Chem.* **1991**, *34*, 3114.

(17) Callahan, J. F.; Bean, J. W.; Burgess, J. L.; Eggleston, D. S.; Hwang, S. M.; Kopple, K. D.; Koster, P. F.; Nichols, A.; Peishoff, C. E.; Samanen, J. M.; Vasko, J. A.; Wong, A.; Huffman, W. F. *J. Med. Chem.* **1992**, *35*, 3970.

(18) Gurrath, M.; Müller, G.; Kessler, H.; Aumailley, M.; Timpl, R. *Eur. J. Biochem.* **1992**, *210*, 911.

(19) Peishoff, C. E.; Ali, F. E.; Bean, J. W.; Calvo, R.; D'Ambrosio, C. A.; Eggleston, D. S.; Hwang, S. M.; Kline, T. P.; Koster, P. F.; Nichols, A.; Powers, D.; Romoff, T.; Samanen, J. M.; Stadel, J.; Vasko, J. A.; Kopple, K. D. *J. Med. Chem.* **1992**, *35*, 3962.

(20) Bogusky, M. J.; Naylor, A. M.; Pitzenberger, S. M.; Nutt, R. F.; Brady, S. F.; Colton, C. D.; Sisko, J. T.; Anderson, P. S.; Veber, D. F. *Int. J. Pept. Protein Res.* **1992**, *39*, 63.

(21) McDowell, R. S.; Gadek, T. R. *J. Am. Chem. Soc.* **1992**, *114*, 9245.

(22) Ku, T. W.; Ali, F. E.; Barton, L. S.; Bean, J. W.; Bondinell, W. E.; Burgess, J. L.; Callahan, J. F.; Calvo, R. R.; Chen, L.; Eggleston, D. S.; Gleason, J. G.; Huffman, W. F.; Hwang, S. M.; Jakas, D. R.; Karash, C. B.; Kennan, R. M.; Dopple, K. D.; Miller, W. H.; Newlander, K. A.; Nichols, A.; Parker, M. F.; Peishoff, C. E.; Samanen, J. M.; Uzinskas, I.; Venslavsky, J. W. *J. Am. Chem. Soc.* **1993**, *115*, 8861.

(23) Sanderson, P. N.; Glen, R. C.; Payne, A. W. R.; Hudson, B. D.; Heide, C.; Tranter, G. E.; Doyle, P. M.; Harris, C. J. *Int. J. Pept. Protein Res.* **1994**, *43*, 588.

(24) Kieffer, B.; Mer, G.; Mann, A.; Lefèvre, J.-F. *Int. J. Pept. Protein Res.* **1994**, *44*, 70.

(25) Pfaff, M.; Tangemann, K.; Müller, B.; Gurrath, M.; Müller, G.; Kessler, H.; Timpl, R.; Engel, J. *J. Biol. Chem.* **1994**, *269*, 20233.

(26) Haubner, R.; Gratias, R.; Diefenbach, B.; Goodman, S. L.; Jonczyk, A.; Kessler, H. *J. Am. Chem. Soc.* **1996**, *118*, 7461.

(27) Haubner, R.; Schmitt, W.; Hölzemann, G.; Goodman, S. L.; Jonczyk, A.; Kessler, H. *J. Am. Chem. Soc.* **1996**, *118*, 7881.

(28) Wermuth, J.; Goodman, S. L.; Jonczyk, A.; Kessler, H. *J. Am. Chem. Soc.* **1997**, *119*, 1328.

(29) Ojima, I.; Chakravarty, S.; Dong, Q. *Bioorg. Med. Chem.* **1995**, *3*, 337.

(30) Burgess, K.; Lim, D.; Mousa, S. A. *J. Med. Chem.* **1996**, *39*, 4520.

<sup>⊗</sup> Abstract published in *Advance ACS Abstracts*, September 15, 1997.

(1) Kopple, K. D. *Biopolymers* **1971**, *10*, 1139.

(2) Deber, C. M.; Madison, V.; Blout, E. R. *Acc. Chem. Res.* **1976**, *9*, 106.

(3) Kessler, H. *Angew. Chem., Int. Ed. Engl.* **1982**, *21*, 512.

(4) Prochazka, Z.; Lebl, M.; Barth, T.; Hlavacek, J.; Trka, A.; Budesinsky, M.; Jost, K. *Czech. Chem. Commun.* **1984**, *49*, 642.

(5) Kessler, H.; Gülzemann; Zechel, C. *Int. J. Pept. Protein Res.* **1984**, *25*, 267.

(6) Stammer, C. H. *Tetrahedron* **1990**, *46*, 2231.

(7) Burgess, K.; Ho, K.-K.; Moye-Sherman, D. *Synlett* **1994**, 8, 575.

(8) Bailie, J. R.; Walker, B.; Nelson, J.; Murphy, R. F. *Int. J. Pept. Protein Res.* **1994**, *43*, 225.

(9) Burgess, K.; Ho, K.-K.; Pettitt, B. M. *J. Am. Chem. Soc.* **1994**, *116*, 799.

(10) Burgess, K.; Ho, K.-K.; Pettitt, B. M. *J. Am. Chem. Soc.* **1995**, *117*, 54.

(11) Burgess, K.; Ho, K.-K.; Pal, B. *J. Am. Chem. Soc.* **1995**, *117*, 3808.

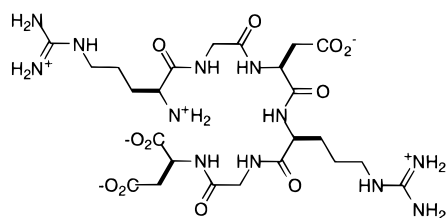
(12) Burgess, K.; Li, W.; Lim, D.; Moye-Sherman, D. *Biopolymers* **1997**, *43*, 439.

(13) Burgess, K.; Ke, C.-Y. *Int. J. Pept. Protein Res.* **1997**, *49*, 201.

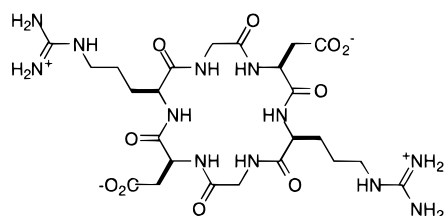
(14) Burgess, K.; Ke, C.-Y. *J. Org. Chem.* **1996**, *61*, 8627.

(15) Burgess, K.; Lim, D.; Ho, K.-K.; Ke, C.-Y. *J. Org. Chem.* **1994**, *59*, 2179.

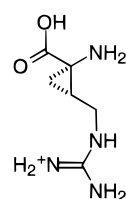
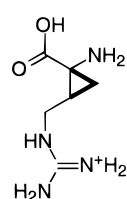
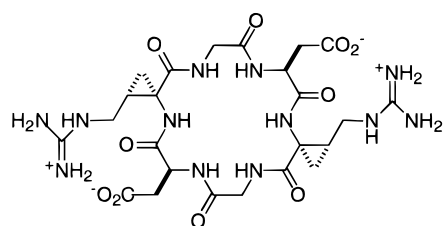
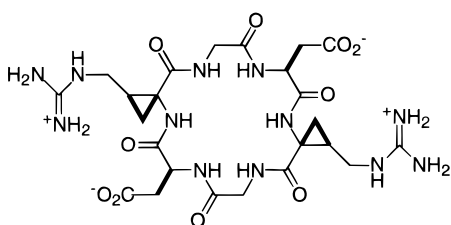
ties of the peptide were in harmony with structure–activity correlations made for other RGD-based systems.<sup>26–28,31</sup>



RGDGRGD 1



cyclo-[RGDGRGD] 2

(2*S*,3*S*)-cyclo-R(2*R*,3*S*)-cyclo-Rcyclo-[(2*S*,3*S*)-cyclo-R]GD[(2*S*,3*S*)-cyclo-R]GD 3cyclo-[(2*R*,3*S*)-cyclo-R]GD[(2*R*,3*S*)-cyclo-R]GD 4

The research described in this paper covers syntheses of the peptidomimetics **3** and **4** and conformational biases of these molecules in solution as ascertained by a combination of CD, NMR, and molecular simulation experiments. Each of these techniques for conformational analysis is considered separately below, and then they are considered collectively to formulate conclusions regarding structural biases. Biological studies which parallel those performed for **2** were also undertaken. Overall, this work is a logical comparison of a cyclic peptide and two spirocyclic peptidomimetics featuring 2,3-methanoamino acids.

(31) Bach, A. C.; Espina, J. R.; Jackson, S. A.; Stouten, P. F. W.; Duke, J. L.; Mousa, S. A.; Degrado, W. F. *J. Am. Chem. Soc.* **1996**, *118*, 293.

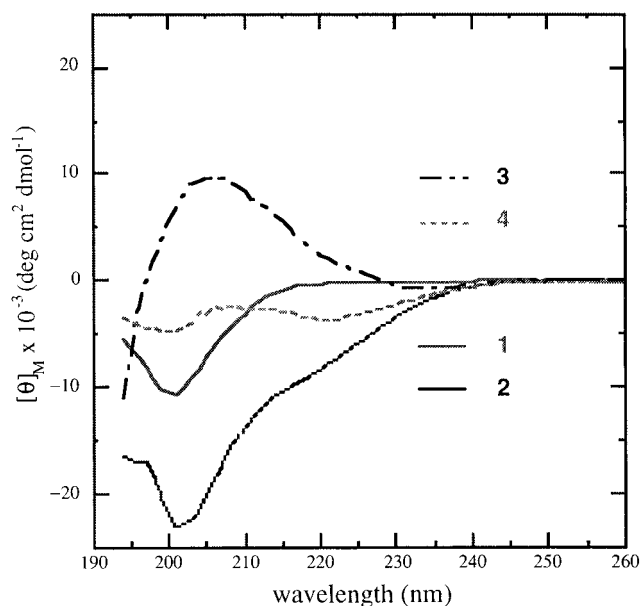


**Figure 1.** Overlaid CD spectra for RGDGRGD (**1**), cyclo-[RGDGRGD] (**2**), cyclo-[(2*S*,3*S*)-cyclo-R]GD[(2*S*,3*S*)-cyclo-R]GD (**3**), and cyclo-[(2*R*,3*S*)-cyclo-R]GD[(2*R*,3*S*)-cyclo-R]GD (**4**).

## Results and Discussion

**Synthesis of 3 and 4.** Various solid phase approaches using Fmoc-protected amino acids<sup>32,33</sup> and PyBOP/HOBt-mediated couplings<sup>34</sup> were investigated for potential syntheses of these molecules. Epimerization complicated the outcome of routes which began with Fmoc-Asp-ODmb (Dmb is 2,4-dimethoxybenzyl)<sup>35</sup> attached to Wang resin via the acid side chain, or Fmoc-Asp(O*t*Bu) attached to 4-methylbenzhydrylamine (MBHA) resin via the highly acid labile 4-(hydroxymethyl)-3-methoxyphenyl butyrate (HMPB) linker.<sup>36</sup> Subsequently, we found that samples in the cyclo-[RGDGRGD] series could be formed without contamination by any significant byproduct via solid phase syntheses beginning with coupling of Gly to HMPB–MBHA resin, elongation of the supported chain, cleavage, cyclization in solution, and then side-chain deprotection. This route avoids epimerization at Asp.

**CD Studies.** Figure 1 shows that the maximum molar ellipticities for **1–4** are in the order  $2 > 3 > 1 > 4$ . Cyclo-[RGDGRGD] (**2**) and cyclo-[(2*S*,3*S*)-cyclo-R]GD[(2*S*,3*S*)-cyclo-R]GD (**3**) would be expected to have more structured amide group environments, and thus stronger CD signals, than RGDGRGD **1**. However, the weak ellipticities observed for cyclo-[(2*R*,3*S*)-cyclo-R]GD[(2*R*,3*S*)-cyclo-R]GD (**4**) were surprising. Interestingly, the ellipticity maximum observed for cyclo-[(2*S*,3*S*)-cyclo-R]GD[(2*S*,3*S*)-cyclo-R]GD (**3**) was opposite to that observed for cyclo[RGDGRGD] (**2**), even though **3** is composed of natural L-amino acids and (2*S*,3*S*)-cyclo-R (which is stereochemically closer to L-Arg than (2*R*,3*S*)-cyclo-R is). One explanation for this would be opposite orientations for some or all of the cyclic backbone amide groups in **3** and **2**.

**One-Dimensional NMR Studies.** Throughout this work, NMR spectra for **2–4** were collected for samples in 50 mM phosphate buffer at pH 5.4. At this pH, the Asp and Arg side chains will be predominantly anionic and cationic, respectively.

(32) Atherton, E.; Sheppard, R. C. *Solid Phase Peptide Synthesis, A Practical Approach*; IRL Press: Oxford, 1989.

(33) Fields, G. B.; Noble, R. L. *Int. J. Pept. Protein Res.* **1990**, *35*, 161.

(34) Coste, J.; Le-Nguyen, D.; Castro, B. *Tetrahedron Lett.* **1990**, *31*, 205.

(35) McMurray, J. S. *Tetrahedron Lett.* **1991**, *32*, 7679.

(36) McMurray, J. S.; Lewis, C. A. *Tetrahedron Lett.* **1993**, *34*, 8059.

**Table 1.** Selected ROE Data for the Cyclic Peptidomimetics in 90% H<sub>2</sub>O–10% D<sub>2</sub>O, pH 5.4, 50 mM Phosphate Buffer

	2 <sup>a</sup>	3 <sup>a</sup>	4 <sup>a</sup>
Arg NH <sup>b</sup> –Gly NH	VW <sup>c</sup>	M	M
Gly NH–Asp NH	VW	VW	VW
Asp NH–Arg NH	W		VW
Arg NH–Asp α	W	S	M
Arg NH–Asp β/β'	VW	VW	VW
Asp NH–Gly α	M	W	W
Asp NH–Gly α'	W	W	W

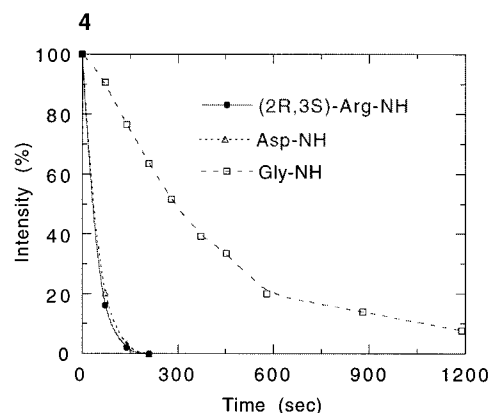
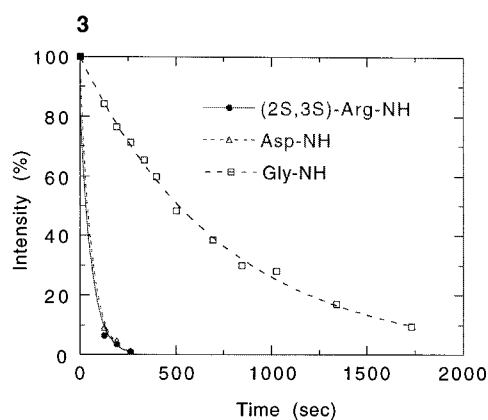
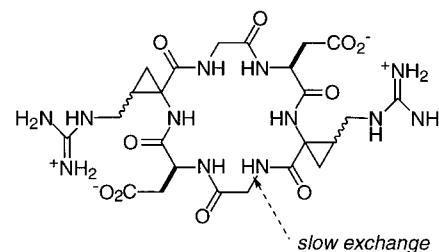
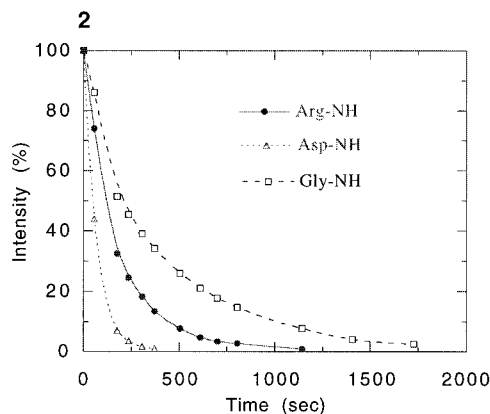
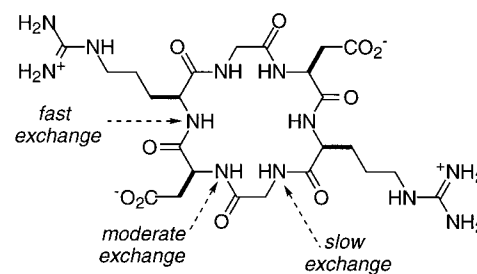
<sup>a</sup> 2 = cyclo-[RGDRGD]; 3 = cyclo-[(2*S*,3*S*)-cyclo-R]GD{(2*S*,3*S*)-cyclo-R}GD; 4 = cyclo-[(2*R*,3*S*)-cyclo-R]GD{(2*R*,3*S*)-cyclo-R}GD].  
<sup>b</sup> In this table, the abbreviation "Arg" is used for L-Arg or cyclo-Arg as appropriate for structures 2–4. <sup>c</sup> S = strong; M = medium; W = weak; VW = very weak.

All the cyclic compounds studied gave only one set of proton NMR signals for the "RGD" component; hence, they either exist in predominantly *C*<sub>2</sub>-symmetric conformations or in non-*C*<sub>2</sub>-symmetric conformations that interconvert rapidly on the NMR time scale. The Gly and Asp NH chemical shifts for 3 and 4 were within 0.55 ppm of those values observed for the corresponding protons in cyclo-[RGDRGD]. However, the Arg NH protons were shifted to significantly lower field in the two spirocyclic peptidomimetics ( $\delta$  ppm, 8.08 for 2, 9.09 for 3, and 9.03 for 4), indicative of a different environment. Coupling constants for the Gly and Asp NH– $\alpha$  spin systems for 3 and 4 were in the range 4.5–6.0 Hz, *i.e.*, less than the value typically associated with random coil conformations (7–8 Hz).<sup>37</sup>

Figure 2 compares the rate of amide proton H/D exchange for 3 and 4. Protons associated with the Gly residues exchange much slower than the others. In general, exchange rates for Gly NH protons are intrinsically slower than those for the other protein amino acids;<sup>38</sup> but for 3 and 4, the rate of N<sub>α</sub>H exchange of the Gly NH was even slower than that for the Gly NH protons in cyclo[RGDRGD] (2). This implies that the solvent shielding/intramolecular H-bonding effects for the parent peptide are different from those of the spiropeptides and that the cyclo-Arg NH protons in the spiropeptidomimetics are least likely to be solvent shielded or intramolecularly hydrogen bonded.

In general, temperature coefficient data<sup>39–41</sup> for peptides/peptidomimetics in aqueous solutions are very hard to interpret. Similar experiments are informative when DMSO is the solvent,<sup>42,43</sup> but H-bonding effects in aqueous systems are much more complicated. Consistent with this, temperature coefficient data were collected for peptidomimetics 2–4 (Supporting Information) but were not easily interpreted.

**Two-Dimensional NMR Studies.** Selected ROE<sup>44</sup> data for 2–4 are shown in Table 1. Quantitative interpretation of ROE data is less reliable than for NOE studies, but trends for this series of compounds having similar structures and almost identical molecular masses are informative. Relative to the parent cyclic peptide 2, cyclo-[(2*S*,3*S*)-cyclo-R]GD{(2*S*,3*S*)-cyclo-R}GD] (3) has stronger cyclo-Arg NH–Asp  $\alpha$  and cyclo-

**Figure 2.** Rate of H/D exchange of amide protons (25 °C in D<sub>2</sub>O): cyclo-[RGDRGD] (2); cyclo-[(2*S*,3*S*)-cyclo-R]GD{(2*S*,3*S*)-cyclo-R}GD] (3); and cyclo-[(2*R*,3*S*)-cyclo-R]GD{(2*R*,3*S*)-cyclo-R}GD] (4).

(37) Wüthrich, K. *NMR of Proteins and Nucleic Acids*; Wiley: New York, 1986.

(38) Dempsey, C. E. *J. Am. Chem. Soc.* **1995**, *117*, 7526.

(39) Stevens, E. S.; Sugawara, N.; Bonora, G. M.; Toniolo, C. *J. Am. Chem. Soc.* **1980**, *102*, 7048.

(40) Stevens, E. S.; Sugawara, N.; Bonora, G. M.; Toniolo, C. *J. Am. Chem. Soc.* **1980**, *102*, 7048.

(41) Kessler, H.; Bats, J. W.; Griesinger, C.; Koll, S.; Will, M.; Wagner, K. *J. Am. Chem. Soc.* **1988**, *110*, 1033.

(42) Kopple, K. D.; Ohnishi, M.; Go, A. *J. Am. Chem. Soc.* **1969**, *91*, 4264.

(43) Ohnishi, M.; Urry, D. W. *Biochem. Biophys. Res. Commun.* **1969**, *36*, 194.

(44) Bothner-By, A. A.; Stephen, R. L.; Lee, J.; Warren, C. D.; Jeanloz, R. W. *J. Am. Chem. Soc.* **1984**, *106*, 811.

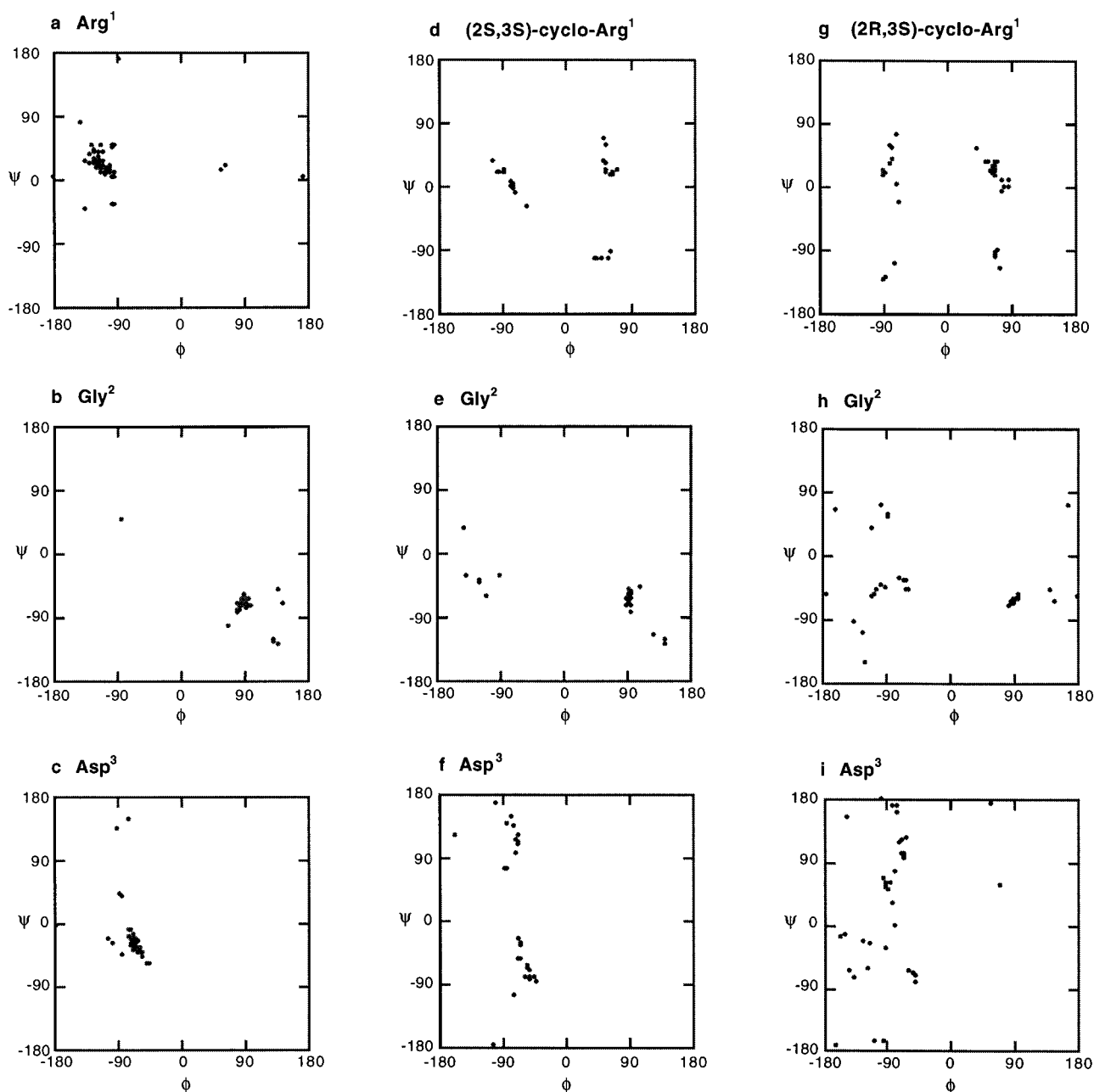


**Figure 3.**  $\phi, \psi$  dot plots generated in a QMD simulation of (a–c) cyclo-[RGDRGD] (**2**); d–f cyclo-[(2*S*,3*S*)-cyclo-R]GD{(2*S*,3*S*)-cyclo-R}GD (**3**); and (g–i) cyclo-[(2*R*,3*S*)-cyclo-R]GD{(2*R*,3*S*)-cyclo-R}GD (**4**). For **2**, most of the conformers have similar  $\phi, \psi$  bond angles, so a single averaged structure is expected. Conformers of **3** cluster in three  $\phi, \psi$  regions for the cyclo-Arg residue, one for the Gly, and two for the Asp, indicative of six significant conformers. Many conformers are possible for **4**.

**Table 2.** Structural Characteristics of the Averaged Low-Energy Conformers from Each of the Families Generated in the QMD Study of cyclo-[(2*S*,3*S*)-cyclo-R]GD{(2*S*,3*S*)-cyclo-R}GD (**3**)

residue	dihedral angle	F1	F2a	F2b	F3	F4
(2 <i>S</i> ,3 <i>S</i> )-cyclo-Arg	$\phi$	57	58	-83	57	-80
	$\psi$	46	24	15	-97	11
Gly	$\phi$	97	116	92	-130	114
	$\psi$	-51	-88	-68	-21	-97
Asp	$\phi$	-81	-70	-59	-95	-63
	$\psi$	94	124	-54	138	-46
no. of members in each family		4	15	3	8	
average energy (kcal/mol <sup>-1</sup> )		-23.46	-23.34	-21.96	-22.74	

Arg NH–Gly NH cross peaks. Cyclo-[(2*R*,3*S*)-cyclo-R]GD{(2*R*,3*S*)-cyclo-R}GD (**4**) also has significant cross peaks for these two contacts, but the difference between **3** and **2** is less

than that between **4** and **2**. Other differences in the ROESY spectra of the three compounds exist, but they are less pronounced. Overall, these data indicate that **2** and **3** have appreciable conformational differences, while **4** is intermediate between the two.

**Molecular Simulations.** The cyclic systems **2–4** are  $C_2$ -symmetric structures. This molecular characteristic makes it easy to identify stable non- $C_2$  symmetric conformers by NMR, and none were observed (*vide supra*). It also means that the number of cross peaks observed for these molecules was about half those for cyclic hexapeptides lacking  $C_2$  symmetry elements. The paucity of data is especially inconvenient for the spirocyclic systems because the methanoarginine residues have no  $C_\alpha H$  protons.

Quenched molecular dynamics (QMD) simulations<sup>45,46</sup> were used in this research since methods based on distance geometry considerations are unsuitable for molecules that are significantly

**Table 3.** Structural Characteristics of the Averaged Low-Energy Conformers from Each of the Families Generated in the QMD Study of cyclo-[(2*R*,3*S*)-cyclo-R]GD{(2*R*,3*S*)-cyclo-R}GD] (**4**)

residue	dihedral angle	F1	F2a	F2b	F3	F4a	F4b	F5	F6	F7
(2 <i>R</i> ,3 <i>S</i> )-cyclo-Arg	$\phi$	64	68	-90	-82	80	-127	53	21	-62
	$\psi$	28	20	25	38	11	13	-7	2	25
Gly	$\phi$	94	94	88	85	34	-7	-145	-117	-161
	$\psi$	-56	-61	-62	-67	-86	23	-37	-64	-25
Asp	$\phi$	-68	-72	-53	-101	43	-133	-101	-106	-165
	$\psi$	102	120	-69	-34	-4	-35	62	103	-143
no. of members in each family		16	7		4	6		7	8	4
average energy (kcal/mol <sup>-1</sup> )		-15.22	-14.23		-13.45	-15.06		-14.02	-13.92	-14.84

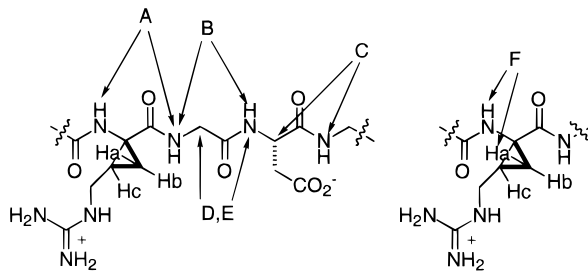
affected by conformational averaging.<sup>47</sup> The QMD approach provides structural representations *before* constraints from NMR are considered, so NMR data that are wholly or partially perturbed by conformational averaging do not lead to erroneous simulations.

Details of the QMD simulation of cyclo-[RGDRGD] have already been published.<sup>30</sup> Those data indicate that the peptidomimetic adopts a single predominant conformational state with a type I  $\beta$ -turn between the NH and CO groups of opposite Gly residues in the ring and  $\gamma$ -turns centered about the Gly residues.

A QMD simulation of cyclo-[(2*S*,3*S*)-cyclo-R]GD{(2*S*,3*S*)-cyclo-R}GD] (**3**) indicates that several conformational states are open to this molecule. This is evident from the  $\phi, \psi$  dot plots of the lowest energy structures generated from the QMD procedure. These  $\phi, \psi$  dot plots are compared for **2** and **3** in Figure 3. Minimized structures for the Arg residue in cyclo-[RGDRGD] (**2**) cluster in one region of conformational space for all three amino acids (Arg, Gly, Asp), but conformations of cyclo-[(2*S*,3*S*)-cyclo-R]GD{(2*S*,3*S*)-cyclo-R}GD] (**3**) occupy three distinct regions of  $\phi, \psi$  about the cyclo-Arg residue and two about the Asp residue. Thus, realistic grouping of the low-energy structures should generate a minimum of three distinct conformational families for **3**, and six conformational families would be reasonable. Several grouping methods were tested (see Experimental Section), and one was selected, giving the four families outlined in Table 2. Family 2 was not  $C_2$  symmetric, so the two RGD components were considered separately, as F2a and F2b. All the other families were  $C_2$  symmetric. Families 1 and 2a were very similar; for instance, none of the backbone  $\phi, \psi$  angles for the consensus (averaged) conformations represented by these families differed by more than 37°.

Figure 3 also shows  $\phi, \psi$  dot plots for the low-energy structures generated in the QMD simulation of cyclo-[(2*R*,3*S*)-cyclo-R]GD{(2*R*,3*S*)-cyclo-R}GD] (**4**). Comparison of the data indicated that more conformations were accessible to **4** than for **3**. In fact, the QMD study of **3** gave only 34 conformers within 6 kcal/mol of the lowest energy conformer identified (*cf.* Table 2), but 52 conformers were within 4 kcal/mol of the lowest energy one found in the QMD study of **4** (*cf.* Table 3). Consequently, the energy minimum located for **3** was narrow and deep relative to that found for **4**. Table 3 shows that seven families were selected for **4**, of which two (families 2 and 4) were not  $C_2$  symmetric. Comparison of the backbone dihedrals for these seven families showed that families 1 and 2a were very similar.

**Formulation of Conformational Models from the CD, NMR, and QMD Studies.** Table 4 shows ROE cross peak

**Table 4.** ROE Cross Peak Intensities and Interproton Distances from Consensus Structures Generated from Each QMD Family for cyclo-[(2*S*,3*S*)-cyclo-R]GD{(2*S*,3*S*)-cyclo-R}GD] (**3**)<sup>a</sup>


contact	ROE intensity	distance calculated from QMD (Å)				
		F1	F2a	F2b	F3	F4
A	M	2.97	2.91	2.94	<b>4.37</b>	2.89
B	VW	3.03	3.44	3.68	<b>1.77</b>	3.87
C	S	1.95	2.00	<b>3.43</b>	2.11	<b>3.38</b>
D	W	2.47	2.33	<b>2.10</b>	2.87	<b>2.00</b>
E	W	3.35	3.45	3.32	3.22	3.24
F	M	2.32	2.39	3.24	2.38	3.16
average $\phi, \psi$ of (2 <i>S</i> ,3 <i>S</i> )-Arg (deg)		57, 46	58, 24	-83, 15	57, -97	-80, 11
no. in family		4	15	3	8	
average energy (kcal mol <sup>-1</sup> )		-23.4	-23.3	-22.0	-22.7	

<sup>a</sup> Discrepancies between the ROE and simulated distances are shown in bold.

intensities for cyclo-[(2*S*,3*S*)-cyclo-R]GD{(2*S*,3*S*)-cyclo-R}GD] (**3**) and interproton distances for consensus structures generated from each QMD family in the appropriate simulation. Interproton distances that do not match the ROE data well are highlighted in bold font. The correspondence between the ROE data and the simulated distances is excellent for families F1 and F2a. There are discrepancies for each of the other families, including at least one serious violation in which the ROE is stronger than predicted on the basis of the simulated distance; this is a more serious type of violation than ones in which the ROE is less than predicted. There are few differences between the consensus structures represented by families F1 and F2a (Table 2, maximum dihedral difference is 37°). Family F2a is derived from non- $C_2$ -symmetric simulated structures wherein the other part of the virtual conformation (F2b) does not fit the ROE data well. Overall, 19 of the 34 lowest energy structures contain an RGD conformation which fits that in F1 (or F2a), and the structures which contain this motif are, on average, the very lowest in energy of those detected in the QMD analysis.

Overlay plots for family 1 in the QMD simulation of **3** are shown in Figure 4. The molecule contains three interlocked turn elements: a type II  $\beta$ -turn between the Gly<sup>1</sup> carbonyl and the Gly<sup>4</sup> NH, a  $\gamma$ -turn centered around the Gly residues, and a type I'  $\beta$ -turn between the Asp<sup>1</sup> carbonyl and the Asp<sup>3</sup> NH. The postulated presence of the type II  $\beta$ -turn is supported by the CD studies, which give a significant positive ellipticity at

(45) Pettitt, B. M.; Matsunaga, T.; Al-Obeidi, F.; Gehrig, C.; Hruby, V. J.; Karplus, M. *Biophys. J. Biophys. Soc.* **1991**, *60*, 1540.

(46) O'Connor, S. D.; Smith, P. E.; Al-Obeidi, F.; Pettitt, B. M. *J. Med. Chem.* **1992**, *35*, 2870.

(47) Wright, P. E.; Dyson, H. J.; Lerner, R. A. *Biochemistry* **1988**, *27*, 7167.

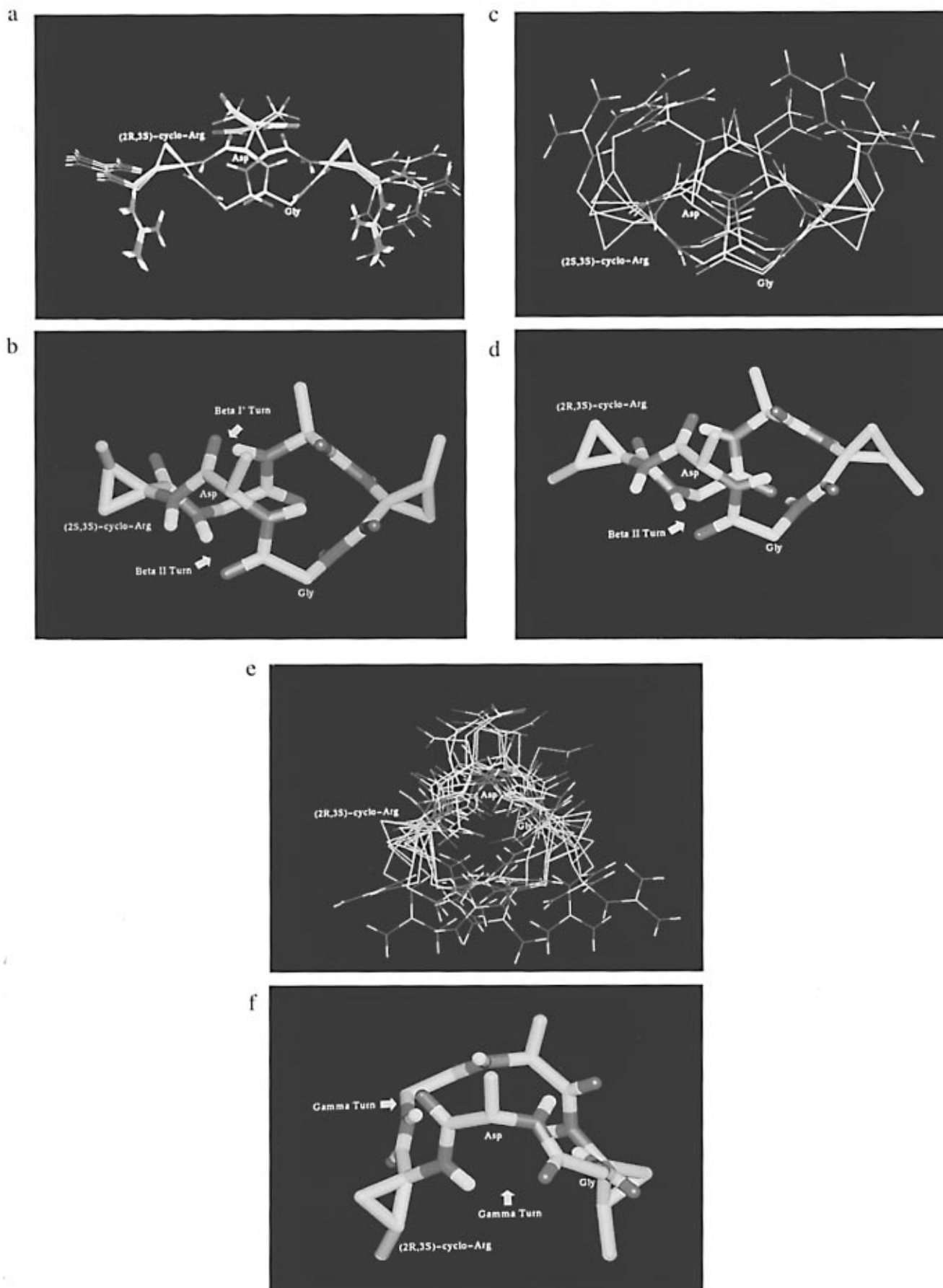


**Figure 4.** Plots from the QMD simulation: (a) overlay of family 1 (F1) for cyclo-[(2S,3S)-cyclo-R]GD{(2S,3S)-cyclo-R}GD (**3**); (b) averaged structure of F1 for **3**; (c) overlay of F1 for cyclo-[(2R,3S)-cyclo-R]GD{(2R,3S)-cyclo-R}GD (**4**); (d) averaged structure of F1 for **4**; (e) overlay of F5 for **4**; (f) averaged structure of F5 for **4**. It is proposed that a and b represent the predominant conformation for **3** and that **4** exists in a series of conformers including those shown in c/d and e/f.

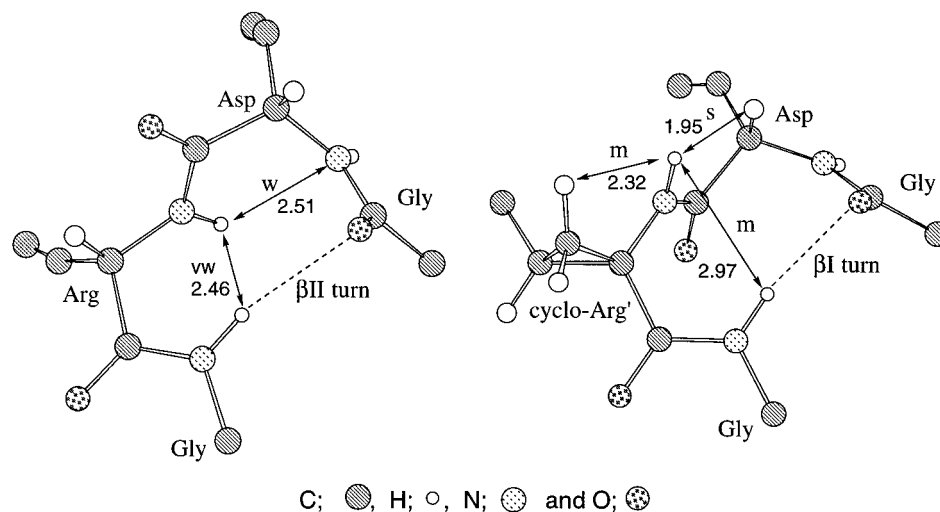
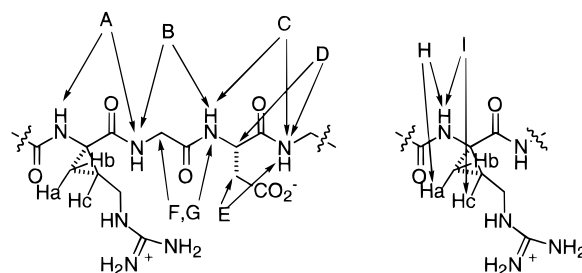


**Figure 5.** Key local interproton distances from averaged structures generated in the QMD simulations and observed ROE intensities for cyclo-[RGDRGD] (**2**) and cyclo-[(2*R*,3*S*)-cyclo-R]GD{(2*S*,3*S*)-cyclo-R}GD] (**3**).

**Table 5.** ROE Cross Peak Intensities and Interproton Distances from Consensus Structures Generated from Each QMD Family for cyclo-[(2*R*,3*S*)-cyclo-R]GD{(2*R*,3*S*)-cyclo-R}GD] (**4**)<sup>a</sup>



contact	ROE intensity	distance calculated from QMD (Å)									
		F1	F2a	F2b	F3	F4a	F4b	F5	F6	F7	
A	M	2.76	2.83	3.07	3.23	2.72	3.11	3.24	3.02	3.05	
B	VW	3.25	3.40	3.39	3.47	2.29	2.53	2.46	2.48	<b>1.90</b>	
C	VW	4.31	4.46	3.11	<b>2.06</b>	<b>2.12</b>	<b>2.13</b>	3.21	3.41	3.74	
D	M	2.03	2.02	3.52	3.46	3.23	3.18	2.29	2.15	2.54	
W	VW	3.95	3.86	3.04	3.67	4.26	3.04	3.98	3.73	2.86	
F	W	2.47	2.39	2.42	2.26	2.86	2.25	2.73	2.22	2.38	
G	W	3.47	3.47	3.47	3.35	3.55	2.81	3.45	3.16	2.67	
H	W	3.22	3.23	2.71	2.49	3.31	2.86	2.91	2.31	2.11	
I	S	2.41	2.38	<b>3.36</b>	<b>3.20</b>	2.36	<b>3.24</b>	2.24	2.30	2.33	
average $\phi, \psi$ of (2 <i>R</i> ,3 <i>S</i> )-Arg (deg)		64, 28	68, 20	-90, 25	-82, 38	80, 11	-127, -13	53, 7	21, 2	-62, 25	
no. in family		16	7		4	6		7	8	4	
average energy (kcal mol <sup>-1</sup> )		-15.2	-14.2		-13.4	-15.1		-14.0	-13.9	-14.8	

<sup>a</sup> Discrepancies between the ROE and simulated distances are shown in bold.

approximately 207 nm. Positive ellipticities at approximately this wavelength have been associated with type II  $\beta$ -turns.<sup>48</sup>

The discussion above indicates that the preferred conformation of **3** is unlike that previously determined<sup>30</sup> for cyclo-[RGDRGD] (**2**). Further support for this conclusion was obtained by comparing the local contacts for the  $\beta$ -turn regions in the simulated structures of **2** and **3**. Results for this comparison are presented in Figure 5. Throughout, the simulated differences and the ROE cross peak intensities correspond to the proposed structural elements.

Matching of the ROE data with the simulated structures for cyclo-[(2*R*,3*S*)-cyclo-R]GD{(2*R*,3*S*)-cyclo-R}GD] (**4**) was expected to be less clear-cut than for **3** because there are more conformers open to the former molecule (*vide supra*, Table 3). The actual extent of correspondence is illustrated in Table 5. No serious violations are observed for families F1, F2a, F5,

and F6, although the fit of the NMR data is not as good for F5 and F6. Consensus structures for families F1 and F2a are very similar (Figure 4): both have conformations in which the Asp and Arg side chains are on opposite faces of the plane formed by the backbone. Consequently, these two charged side chains are not well disposed to maximize electrostatic interactions between them. Unlike F1 and F2a, families 5 (Figure 4) and 6 both have inverse  $\gamma$ -turn motifs about the Asp residue. These correspond to the negative/positive quadrant  $\phi, \psi$  conformational space, which the QMD study indicates is populated for this molecule (Figure 3). The backbone conformations in families F1/F2a and F5/F6 are different; hence, the simulations indicate that conformational averaging between dissimilar conformational states may occur. This inference is consistent with the lack of CD ellipticity observed for **4** (Figure 1).

**Receptor Binding Studies.** The peptidomimetics produced in this study were tested for their ability to disrupt the  $\alpha$ V $\beta$ 3-vitronectin and GPIIb/IIIa-fibrinogen interaction. Data from the

(48) Kitagawa, O.; Velde, D. V.; Dutta, D.; Morton, M.; Takusagawa, F.; Aubé, J. *J. Am. Chem. Soc.* **1995**, *117*, 5169.

same assays have already been reported for **1** and **2**.<sup>30</sup> The spirocyclic peptides were significantly less active than these compounds. Cyclo-[(2*S*,3*S*)-cyclo-R]GD{(2*S*,3*S*)-cyclo-R}GD] (**3**) at 10  $\mu$ M concentration showed only 9% inhibition of the  $\alpha$ V $\beta$ 3-vitronectin interactions, and cyclo-[(2*R*,3*S*)-cyclo-R]GD{(2*R*,3*S*)-cyclo-R}GD] (**4**) showed 52% inhibition under the same conditions. As a reference, D-2-aminobutyroxy-*N*-methyl-L-arginyl-glycyl-L-aspartyl)-3-aminomethylbenzoic acid,<sup>49,50</sup> tested simultaneously in this same assay, gave a 50% inhibition at 20 nM concentration. Neither **3** nor **4** showed any detectable inhibition of the GPIIb/IIIa-fibrinogen interaction.

**Conclusions.** Results presented in this paper imply that cyclo-[(2*S*,3*S*)-cyclo-R]GD{(2*S*,3*S*)-cyclo-R}GD] (**3**) has a relatively clear conformational preference for a structure with three interlocking turn elements. The intrinsic bias of 2,3-methanoamino acids toward  $\gamma$ -turn conformations, which we have suggested on the basis of other studies with linear peptidomimetics,<sup>9–11,14</sup> is apparently overridden in **3** by the cyclization constraints. Like cyclo-[RGDRGD] (**2**),<sup>30</sup> molecule **3** has a  $\beta$ -turn between the CO and the NH of the two Gly residues in the large ring and  $\gamma$ -turns centered on the same glycines. However, the  $\beta$ -turn type is  $\beta$ I for **2** and  $\beta$ II for **3**, meaning that the amide bond between the  $i + 1$  and  $i + 2$  residues adopts opposite orientations. This conformational difference may explain why the CD spectra of the two molecules are so different. Switching between two  $\beta$ -turn types can have a profound effect on the receptor binding affinities for RGD peptidomimetics,<sup>31,51</sup> and in this work **3** (postulated  $\beta$ II turn) binds less strongly than **2** ( $\beta$ I turn). Selectivity for the  $\alpha$ V $\beta$ 3 receptor has been associated with relatively close orientation of the Arg and Asp side chains.<sup>31,51</sup> Such conformations are possible for cyclo-[(2*S*,3*S*)-cyclo-R]GD{(2*S*,3*S*)-cyclo-R}GD] (**3**); however, it has a weak affinity for that receptor, presumably due to an unfavorable backbone conformation.

Cyclo-[(2*R*,3*S*)-cyclo-R]GD{(2*R*,3*S*)-cyclo-R}GD] (**4**) has a conformational bias which is different from that of **3**. Lack of detectable activity for this compound can be attributed to the fact that the Asp and Arg side chains tend to be oriented on different faces of the cyclic backbone system. This unfavorable disposition of the oppositely charged groups also accounts for the greater mobility of the peptide system, which seems to sample other conformational states to decrease the electrostatic energy of the molecule. Like **3**, **4** has only a weak affinity for the  $\alpha$ V $\beta$ 3 receptor.

$\alpha$ V $\beta$ 3 receptor binding affinities in this research are such that **2** > **4** > **3**. One possible explanation for this observation is that, in **3**, the Asp and Arg side chains of consecutive residues (*i.e.*, Asp<sup>3</sup>/Arg<sup>4</sup> and Asp<sup>6</sup>/Arg<sup>1</sup>) are held relatively close together. Binding to the  $\alpha$ V $\beta$ 3 receptor may require that this artificial electrostatic constraint be overcome, and the docking event might, therefore, be relatively unfavorable.

This study illustrates cases wherein 2,3-methanoamino acids incorporated into cyclic systems tend to preclude ideal bioactive conformations. Other stereoisomers of 2,3-methanoarginine will probably impose different conformations. It should be possible to design molecules which are constrained to adopt favorable orientations for biomolecular interactions as the data set for predicting the conformational bias of peptidomimetics based on these 2,3-methanoamino acids becomes greater. Molecular

modeling studies to predict the best 2,3-methanoarginine isomers to obtain  $\alpha$ V $\beta$ 3 receptor selectivities are now plausible.

## Experimental Section

**Synthesis of cyclo-[(2*S*,3*S*)-cyclo-R]GD{(2*S*,3*S*)-cyclo-R}GD] (**3**).** Stepwise couplings of Fmoc-amino acid derivatives on HMPB-MBHA resin were used to prepare a linear precursor, which was then cyclized off the resin. A scheme summarizing this synthesis is given in the Supporting Information. Thus, manual peptide synthesis was carried out in a 30 mL vessel fitted with a coarse glass frit using a wrist action shaker (Burrel, Model 75). The reagents were added manually. All reactions were carried out at 25 °C unless otherwise specified. Fmoc deprotection was performed by shaking the resin twice with 20% piperidine in DMF (5 mL, 3 min and 5 mL, 7 min); DMF washing cycles (10  $\times$  1 min, *ca.* 10 mL) were performed after each coupling and deprotection. The coupling conditions were as follows. The symmetric anhydride of Fmoc-Gly-OH was prepared by mixing 0.339 g of the amino acid derivative (1.14 mmol) and diisopropyl carbodiimide (DIPCDI) (89  $\mu$ L, 0.57 mmol) in CH<sub>2</sub>Cl<sub>2</sub> (4 mL). The mixture was stirred for 1 h and used for coupling without purification. HMPB-MBHA resin (200 mg of 0.57 mmol g<sup>-1</sup> capacity, NovaBiochem) was swelled in DMF (*ca.* 10 mL) for 1 h and then reacted with (Fmoc-Gly)<sub>2</sub>O (0.57 mmol, 5 equiv) and DMAP (28 mg, 0.228 mmol) in DMF (5 mL). The mixture was stirred for 19 h at 25 °C, and the resin was washed. The Fmoc protecting group was removed, and the resin was washed as previously. Five cycles of deprotection and coupling were then performed. The 4-methoxy-2,3,6-trimethylbenzenesulfonyl (Mtr) group was used as side-chain protection for cyclo-arginine (*i.e.*, Fmoc(2*S*,3*S*)-cyclo-Arg(Mtr) was used). The *tert*-butyl (tBu) ester was used for side-chain protection of aspartic acid. For the coupling of the Arg analog, a mixture of Fmoc-(2*S*,3*S*)-cyclo-Arg(Mtr) (69 mg, 0.114 mmol), PyBOP (71 mg, 0.137 mmol), HOBt (19 mg, 0.137 mmol), and NMM (15  $\mu$ L, 0.137 mmol) was used. In the coupling of Asp, freshly preformed Fmoc-Asp(tBu)-F<sup>52</sup> (0.61 mmol, 5.4 equiv) and DIPEA (106  $\mu$ L, 0.61 mmol) in CH<sub>2</sub>Cl<sub>2</sub>-DMF (1:2,  $\sim$ 10 mL) were shaken for 30 min. For the Gly coupling, 4 equiv of each Fmoc-Gly-OH, PyBOP, HOBt, and NMM was mixed. The Fmoc-protected linear peptide was cleaved from the resin using a 1% TFA solution in CH<sub>2</sub>Cl<sub>2</sub> (10  $\times$  2 min, 8 mL), and the cleavage was checked by TLC. The combined solution was concentrated and then added dropwise to the ice-cooled water (60 mL) with stirring. The resulting solid was filtered and dried to give 156 mg of crude peptide. Removal of Fmoc was carried out with a 10% diethylamine solution in CH<sub>3</sub>CN (25 mL). After stirring for 2.5 h at 25 °C, the reaction solution was concentrated, and CH<sub>3</sub>CN (20 mL) was added and evaporated twice to remove traces of diethylamine and then triturated with Et<sub>2</sub>O to remove the dibenzofulvene produced. After filtration and washing with Et<sub>2</sub>O, 121 mg of a white solid was obtained. Cyclization of this peptide was performed using BOP (354 mg, 8.0 equiv), HOBt (108 mg, 8 equiv), and DIPEA (140  $\mu$ L, 8 equiv) in DMF (100 mL, 1 M concentration). After being stirred for 4 days, the reaction solution was concentrated, poured into H<sub>2</sub>O, and extracted with EtOAc. After being washed with water and brine and then dried over MgSO<sub>4</sub>, the organic layer was concentrated to give the crude cyclized product as a white solid.

Deprotection of the side chains and purification of the peptide was performed as follows. A mixture of phenol (0.5 mL), 1,2-ethanedithiol (0.25 mL), thioanisole (0.5 mL), deionized water (0.5 mL), and trifluoroacetic acid (8.25 mL) was cooled to 0 °C and added to the cyclic peptide. The reaction mixture was stirred for 48 h at 25 °C and then concentrated to dryness. Et<sub>2</sub>O (30 mL) was added to precipitate the product, and then the ethereal solution was decanted away from the solid residue. The crude peptide was further purified by preparative RP-HPLC (Vydac C18 column, 22 mm  $\times$  25 cm, 10  $\mu$ m), with a linear gradient obtained by mixing solvent A (0.1% TFA in water) and solvent B (0.1% TFA in acetonitrile). The gradient was programmed to increase from 3 to 4% B over 30 min with a flow rate of 6 mL min<sup>-1</sup>. The peak with a retention time of 27.3 min was collected and lyophilized. cyclo-[(2*S*,3*S*)-cyclo-R]GD{(2*S*,3*S*)-cyclo-R}GD] (TFA

(49) Mousa, S. A.; Bozarth, J. M.; Forsythe, M. S.; Lorelli, W.; Thoolen, M. J.; Ramachandran, N.; Jackson, S.; Grado, W. D.; Reilly, T. M. *Cardiology* **1993**, *83*, 374.

(50) Mousa, S. A.; Bozarth, J. M.; Forsythe, M. S.; Jackson, S. M.; Leamy, A.; Diemer, M. M.; Kapil, R. P.; Knabb, R. M.; Mayo, M. C.; Pierce, S. K.; Grado, W. F. D.; Thoolen, M. J.; Reilly, T. M. *Circulation* **1994**, *89*, 3.

(51) Müller, G. *Angew. Chem., Int. Ed. Engl.* **1996**, *35*, 2767.

(52) Carpino, L. A.; Sadat-Aalae, D.; Chao, H. G.; DeSelms, R. H. J. *Am. Chem. Soc.* **1990**, *112*, 9651.



salt) was obtained as a hygroscopic powder (10.1 mg, 10% based on the resin used): +FAB/DP (thioglycerol),  $m/z$  calcd for  $C_{24}H_{40}N_{12}O_{10}$  652, found 653 for  $[M + H]^+$ . Details of the proton NMR data of this product are given in Supporting Information Table 1.

**Synthesis of cyclo-[(2R,3S)-cyclo-R]GD{(2R,3S)-cyclo-R}GD(4).** Synthesis of this analog was performed using a protocol similar to the one used for cyclo-[(2R,3S)-cyclo-R]GD{(2R,3S)-cyclo-R}GD(3) except that Fmoc-Asp(Bu)-OH was used for the coupling instead of Fmoc-Asp(Bu)-F. After the solid phase synthesis, cleavage, cyclization, and deprotection, one major isomer was obtained. After preparative HPLC separation ( $t_R = 16.6$  min, 3–8% of B over 24 min), pure product was obtained and characterized by MS and NMR spectroscopy: +FAB/DP (thioglycerol)  $m/z$  calcd for  $C_{24}H_{40}N_{12}O_{10}$  652, found 653 for  $[M + H]^+$ . NMR data of this product are listed in Table 1.

**Molecular Modeling.** CHARMM (version 22, Molecular Simulations Inc.) was used for the molecular simulations performed in this work. Extended atom representations of the nonpolar hydrogen atoms were used. Since the CHARMM 22 does not have parameters for cyclopropyl amino acids as extended atom representations, additional atom types were assigned, and a parameter set was built based on crystallographic data and CHARMM 22 default parameters and then appended to the original parameter set. The residue topology files (RTF) for the two cyclo-Arg' analogs were built as well. Ac-(2S,3S)-cyclo-Arg-NHMe was built and minimized to see any structural deformation and/or conformational awkwardness to test the topology and parameter sets. A grid search was also performed to check the energy surface of the molecule. A  $\phi, \psi$  contour plot for cyclo-Arg showed that the energy surface is complicated by charge interactions between the guanidinium side chain and backbone carbonyl (data not shown), but it was reasonable based on chemical intuition. Residue topology files and parameter sets for the cyclo-Arg system are given in the Supporting Information.

Quenched molecular dynamics simulations were performed using the combined parameters. Thus, the molecules of interest, cyclo-[(2S,3S)-cyclo-R]GD{(2S,3S)-cyclo-R}GD and cyclo-[(2R,3S)-cyclo-R]GD{(2R,3S)-cyclo-R}GD, were built with positive charges on the guanidine side chains and negative charges on the Asp side chains. These starting conformers were minimized using 200 steps of steepest descent (SD) and 1000 steps of the adopted basis Newton–Raphson method (ABNR) in a dielectric continuum of 80 (representing water). The minimized structure was then subjected to heating, equilibration, and dynamics simulation. Throughout, the equations of motion were integrated using the Verlet algorithm with a time step of 1 fs, and SHAKE was used to constrain all bond lengths containing polar hydrogens. Each peptide was heated to 1000 K over 10 ps by increasing the temperature by 10 K every 0.1 ps. The peptide was equilibrated for 10 ps at 1000 K, during which time a  $\pm 13$  K temperature constraint was applied to the system. Molecular dynamics production runs were then performed in the microcanonical (NVE) ensemble for a total time of 1000 ps. The trajectories were saved every 1 ps, and a total of 1000 structures was produced. Each of the structures was thoroughly minimized using 200 steps of SD followed by ABNR until an rms energy derivative of  $\leq 0.0001$  kcal mol $^{-1}$  Å $^{-1}$  was obtained. Extra H-bonding options were applied during the minimization since the high dielectric constant reduces the intramolecular H-bonding contributions to the energy term. If the extra hydrogen bonding energy term was not used, the overall fit with the NMR data was poor.

Structures  $\leq 4$ –6 kcal mol $^{-1}$  of the global minimum were selected for further analyses. For cyclo-[(2S,3S)-cyclo-R]GD{(2S,3S)-cyclo-R}GD(3), a 6 kcal mol $^{-1}$  cutoff was used, giving 34 structures for further analysis. A total of 52 structures were obtained for cyclo-[(2R,3S)-cyclo-R]GD{(2R,3S)-cyclo-R}GD(4) after the 4 kcal mol $^{-1}$  cutoff.

The Quanta 4.0 package was used to display and overlay the selected structures and to group them into families. Many approaches were tested to obtain the best clustering. Simple grouping methods based on the calculation of rms deviation of differently selected atom subsets from the lowest energy structure failed to give reasonably homogeneous families. Consequently, the  $\phi, \psi$  scatter plot of the Arg analog was used as a basis. A reference structure was selected from each quadrant, and then rms deviations were calculated on the basis of the following atoms around the Arg analog: Asp, CO; cyclo-Arg', NH-C $\alpha$ -CO; Gly,

NH. Threshold cutoff values were selected to obtain families with reasonable homogeneity. Some “families” having only one or two structures were not listed in Tables 2 and 3.

The coordinates of each family were reoriented by mass weighting an rms calculation using peptide backbone atoms, averaged in Cartesian coordinates, and the protons were built on the heavy atoms using standard geometries. Finally, the interproton distances were calculated from these coordinates for comparisons of the simulated structures with the ROE data obtained in the NMR studies.

**NMR Studies.** NMR spectra were recorded on a Varian Unity+500 spectrometer (500 MHz). In the COSY/ROESY experiments, selective presaturation was carried out to suppress the water signal. The peptide (4.76 mM) was dissolved in a mixture of 10% D $_2$ O and 90% H $_2$ O containing potassium phosphate (50 mM, pH = 5.5). In the H–D exchange experiments, the peptide was placed in a NMR tube, D $_2$ O was added, and the spectra were recorded at intervals after that.

One-dimensional (1D)  $^1$ H NMR spectra were recorded with a spectral width of 8000 Hz, 32 transients, and a 5 s acquisition time. Vicinal coupling constants were measured from the 1D spectra at ambient temperature. Temperature coefficients of amide protons were measured via several 1D experiments at 5–45 °C, adjusted in 10 °C increments with an equilibration time of  $\geq 10$  min after successive temperature steps.

Two-dimensional (2D) spectra were taken at 25 °C, with a spectral width of 8000 Hz. Through-bond connectivities were elucidated by DQF-COSY spectra,<sup>53</sup> which were recorded with 512  $t_1$  increments and 32 scans per  $t_1$  increment, with 2K data points at  $t_2$ .

Sequential assignments and proton–proton close contacts were elucidated by ROESY spectra,<sup>44</sup> which were recorded with a 1 s relaxation delay, 512  $t_1$  increments, and 32 scans per  $t_1$  increment, with 2K data points at  $t_2$ . The spin-lock field was continuous. The carrier frequency was fixed to water signal, and resonance offset compensation was applied. ROESY experiments were performed with mixing times of 100, 200, 300, and 500 ms for the cyclo-[RGDRGD] to identify peaks caused by spin diffusion; the cross peak intensities were almost identical for the mixing times of 300 and 500 ms. Consequently, a 400 ms mixing time was used for cyclo-[(2S,3S)-cyclo-R]GD{(2S,3S)-cyclo-R}GD(3) and cyclo-[(2R,3S)-cyclo-R]GD{(2R,3S)-cyclo-R}GD(4). Both DQF-COSY and ROESY data were zero-filled to 2K  $\times$  2K data sets and Gaussian transformed in both dimensions. The intensities of the ROESY cross peaks were assigned as VS (very strong), S (strong), M (medium), W (weak), and VW (very weak) by the magnitude of their volume integrals. Cutoff distances from ROE data tend to be less than those in the corresponding NOE experiments.<sup>54</sup> Nevertheless, an upper level constraint of 5 Å is maintained in this study to ensure that the boundary conditions for comparisons of NMR and experimental data are not too severe.

**CD Studies.** The peptides were dissolved in 50 mM potassium phosphate buffer solution (pH 5.4). Concentrations were determined by comparing the HPLC integration at 214 nm detection with that of a RGDRGD sample of exactly determined concentration. The concentration range of the samples studied was 286–456  $\mu$ M. CD spectra were obtained using an Aviv (Model 62DS).

**Acknowledgment.** We thank Shaker A. Mousa of DuPont Merck for running the receptor binding assays. K.B. gratefully acknowledges support from NIH and The Robert A. Welch Foundation, an NIH Research Career Development Award, and The Alfred P. Sloan Foundation for a fellowship. We would like to thank Steve Silber for helpful discussions.

**Supporting Information Available:** Experimental scheme for the synthesis of 3, chemical shift and coupling constant information, parameter sets and topology files for 2,3-methanoarginine, and temperature coefficient data for 2–4 (10 pages). See any current masthead page for ordering and Internet access instructions.

JA971629D

(53) Piantini, U.; Sorensen, O. W.; Ernst, R. R. *J. Am. Chem. Soc.* **1982**, *104*, 6800.

(54) Bauer, C. J.; Frenkiel, T. A.; Lane, A. N. *J. Magn. Reson.* **1990**, *87*, 144.